https://doi.org/10.5194/tc-2020-329
Preprint. Discussion started: 19 November 2020

The Cryosphere Discussions

Sensitivity of the surface energy budget to drifting snow as simulated by MAR in coastal Adelie Land, Antarctica

Louis Le Toumelin[1, 2], Charles Amory[1,3], Vincent Favier[1], Christoph Kittel[3], Stefan Hofer[4], Xavier Fettweis[3], Hubert Gallée[1], and Vinay Kayetha[5]

[1]Université Grenoble Alpes, CNRS, Institut des Géosciences de l'Environnement, 38000, Grenoble, France
[2]Univ. Grenoble Alpes, Université de Toulouse, Météo-France, CNRS, CNRM, Centre d'Études de la Neige, Grenoble, France
[3]F.R.S.-FNRS, Laboratory of Climatology, Department of Geography, University of Liège, 4000 Liège, Belgium
[4]Department of Geosciences, University of Oslo, Oslo, Norway
[5]Science Systems and Applications, Greenbelt, MD, USA

Correspondence: Louis Le Toumelin (louis.letoumelin@gmail.com)

Abstract. In order to understand the evolution of the climate of Antarctica, dominant processes that control surface and low-atmosphere meteorology need to be accurately captured in climate models. We used the regional climate model MAR (v3.11) at 10 km horizontal resolution, forced by ERA5 reanalysis over a 9-year period (2010–2018), to study the impact of drifting snow (designing here the wind-driven transport of snow particles below and above 2 m) on the near-surface atmosphere and surface in Adelie Land, East Antarctica. Two model runs were performed, respectively with and without drifting snow, and compared to half-hourly in situ observations at D17, a coastal and windy location of Adelie Land. We show that sublimation of drifting-snow particles in the atmosphere drives the difference between model runs and is responsible for significant impacts on the near-surface atmosphere. By cooling the low atmosphere and increasing its relative humidity, drifting snow also reduces sensible and latent heat exchanges at the surface (- 5.9 Wm^{-2} on average). Moreover, large and dense drifting-snow layers act as near-surface cloud by interacting with incoming radiative fluxes, enhancing incoming longwave radiations and reducing incoming shortwave radiations in summer (net radiative forcing: 5.9 Wm^{-2}). Even if drifting snow modifies these processes involved in surface-atmosphere interactions, the total surface energy budget is only slightly modified by introducing drifting snow, because of compensating effects in surface energy fluxes. The drifting-snow driven effects are not prominent near the surface but peak higher in the boundary layer (fifth vertical level, 38m) where drifting snow sublimation is the most pronounced. Accounting for drifting snow in MAR generally improves the comparison at D17, more especially for the representation of relative humidity (mean bias reduced from -11.1 % to 2.9 %) and incoming longwave radiation (mean bias reduced from -7.6 Wm^{-2} to -1.5 Wm^{-2}). Consequently, our results suggest that a detailed representation of drifting-snow processes is required in climate models to better capture the near–surface meteorology and surface—atmosphere interactions in coastal Adelie Land.

1 Introduction

In order to improve estimates of the contribution of the Antarctic ice sheet to sea level rise in a global warming scenario (Edwards et al., 2019; Shepherd et al., 2018), an accurate representation of the current surface mass balance (SMB) of the ice

https://doi.org/10.5194/tc-2020-329
Preprint. Discussion started: 19 November 2020


The Cryosphere Discussions

sheet and overlying atmospheric physics in models is necessary (Agosta et al., 2019; van Wessem et al., 2018). A particular feature of the climate of Antarctica is the widespread, wind-driven removal and transport of snow, often referred to as drifting and blowing snow. Both processes are theoretically distinguished by the height of the wind-driven snow particles (below 2 m for drifting snow and above that height for blowing snow). For convenience, in our study drifting and blowing snow are combined into the single term of drifting snow.

Locally, drifting snow has proven itself a key SMB parameter. Even if drifting snow is subject to a high spatial and temporal variability, significant yearly frequency (up to > 90 % of the time) and mass transport values have been reported at various places scattered over the Antarctic continent (e.g., Gossart et al., 2017; Mahesh et al., 2003; Mann et al., 2000; Scarchilli et al., 2010; Amory, 2020), especially in the megadune region and coastal windy regions (Palm et al., 2017, 2018). Over coastal locations, wind-driven ablation (erosion and sublimation of drifting-snow particles) and precipitation can be of the same order of magnitude (Scarchilli et al., 2010; van den Broeke et al., 2006). Drifting snow can spread horizontally over hundreds of kilometers, vertically over hundreds of meters (Palm et al., 2011) and remove by erosion all the accumulated firn at the surface, creating climate-sensitive low-albedo blue-ice areas (Bintanja, 1999; Favier et al., 2011; Scarchilli et al., 2010). At the scale of the Antarctic ice-sheet, model studies even suggest that ablation may be primarily due to drifting snow (Lenaerts and van den Broeke, 2012; van Wessem et al., 2018; Palm et al., 2018), although drifting-snow mass transport could still be underestimated in regional-model-based estimates of the Antarctic SMB (Agosta et al., 2019). Despite these efforts, drifting-snow processes still need to be more accurately resolved in models and better observationally constrained to improve our understanding of their influence on the climate and surface mass balance of Antarctica (Favier et al., 2017; Amory, 2020; Hanna et al., 2020).

Drifting-snow particles influence the local climate through their interactions with the lower atmosphere and the surface energy budget. Latent heat consumption and moisture release through sublimation of wind-driven particles modify the vertical gradients in temperature and humidity (e.g., Schmidt, 1982; Déry et al., 1998; Bintanja, 2000; Amory and Kittel, 2019), further affecting the turbulent heat exchange with the surface (Bintanja, 2001; Lenaerts and van den Broeke, 2012; Barral et al., 2014). Yang et al. (2014) observed through remote sensed data that drifting snow can increase top-of-atmosphere outgoing longwave radiation by more than 20 Wm^{-2} during wintertime in East Antarctica, suggesting a significant contribution of drifting snow to the atmospheric radiative budget. In the cold environment of central Antarctica, the lower atmosphere is usually very dry and clouds are generally optically thin (Mahesh et al., 2003; Town et al., 2007). The surface energy budget is thus particularly sensitive to increases in the atmospheric longwave emissivity caused by additional suspended particles or water vapour due to drifting-snow sublimation. Yamanouchi and Kawaguchi (1984) highlighted increases in downwelling longwave radiation up to 20 Wm^{-2} below 30 m above ground during drifting snow from observations collected at Mizuho Station. The occurrence of drifting-snow layers has been linked to increases in surface temperature of typically a few degrees at South Pole (Mahesh et al., 2003). In a modelling study with the regional climate model MAR, Gallée and Gorodetskaya (2010) showed that neglecting the contribution of suspended snow particles to the atmospheric longwave emissivity resulted in underestimation of the surface temperature at Dome C. Only small rises in surface temperature can be expected on the Antarctic Plateau in response to additional drift-induced radiative forcing due to the strong surface-based temperature inversion that prevails throughout the year. But over coastal areas of the Antarctic ice sheet, which experience stronger wind speeds and related turbulent mixing,

https://doi.org/10.5194/tc-2020-329
Preprint. Discussion started: 19 November 2020

and where higher, optically thicker drifting-snow layers can frequently develop (Palm et al., 2018), radiative effects of drifting snow remain currently poorly documented.

Drifting-snow data are extremely limited over high-latitude regions and still remain challenging to collect in the extreme and remote Antarctic environment (Amory, 2020). Drifting-snow effects are moreover directly embedded in measurable climate quantities and can hardly be disentangled from usual atmospheric measurements without an accurate knowledge of drifting-snow properties in the whole atmospheric column. As an alternative, regional climate models provide continuous, high-resolution gridded estimates of individual climate components over large areas (van Wessem et al., 2018; Agosta et al., 2019). Detailed modelling may thus provide physical insights into the relevance and climatological significance of drifting snow. However, only a few regional models currently explicitly quantify drifting-snow processes (Lenaerts and van den Broeke, 2012; Gallée et al., 2013; Amory et al., 2015, 2020b), and different implementation strategies from one model to another have been employed to account for interactions of drifting snow with the atmosphere (Gallée et al., 2013).

In this paper we use the regional climate model MAR to quantify the influence of drifting snow on the near-surface climate and surface energy budget in Adelie Land, a coastal region of East Antarctica particularly prone to erosive winds and where drifting-snow equipment deployed over the past few years provide observational support for model evaluation near the surface (Trouvilliez et al., 2014; Amory et al., 2020b). MAR has been widely used to simulate the climate and surface mass balance of polar ice sheets (e.g., Fettweis et al., 2013, 2017, 2020; Hofer et al., 2017, 2019; Kittel et al., 2018, 2020; Agosta et al., 2019; Mottram et al., 2020), and includes a detailed representation of drifting-snow processes already applied to study snow mass transport and wind-driven ablation in coastal East Antarctica (Gallée et al., 2005; Gallée et al., 2013; Amory et al., 2015, 2020b). The explicit coupling of the drifting-snow scheme with the atmospheric component of the model enables a vertical discretization of drifting-snow profiles and related sublimation within the atmospheric boundary layer and takes into account the radiative contribution of drifting-snow particles.

Observations, model setup and data processing methods are described in Sect. 2. Main modifications induced by drifting snow on the surface and near-surface meteorology at D17 are detailed in Sect. 3. Sect. 4 discusses the results including the impact of drifting snow on the boundary layer and their spatial distribution in Adelie Land. Finally, Sect. 5 summarizes and concludes the study.

2 Methods and data

2.1 Field area and instrumentation

Site D17 (66.7° S, 139.9° E; 450 m above sea level, Fig. 1) is located 10 km inland and 15 km southwest of the permanent French station of Dumont d'Urville, in Adelie Land, East Antarctica. The measurement area is characterized by strong and persistent katabatic winds mostly originating from the south-east direction and flowing over a permanent snow surface, favouring the regular occurrence of drifting snow (Amory, 2020).

A 7 m meteorological mast has been installed at D17 in 2010 providing relative humidity, wind speed, and temperature measurements at six logarithmically spaced levels (nominal heights 0.8, 1.3, 2, 2.8, 3.9, and 5.5 m above the surface). An

https://doi.org/10.5194/tc-2020-329
Preprint. Discussion started: 19 November 2020

The Cryosphere Discussions
Open Access
EGU

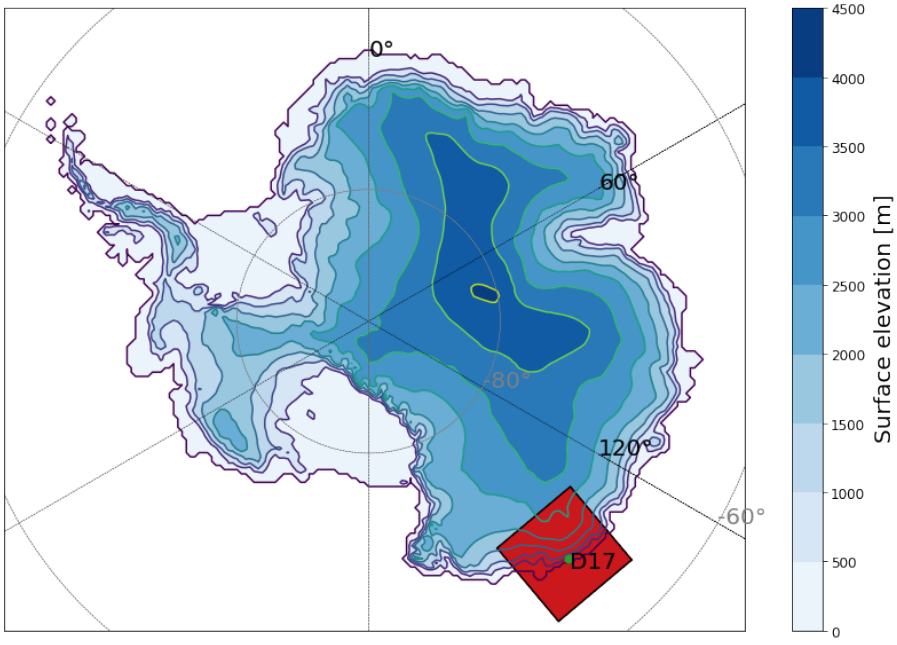

Figure 1. Antarctic topography as used in MAR. The integration domain over Adelie Land is displayed in red with a green dot for D17 location.

ultrasonic depth gauge measures changes in elevation above ground level since December 2012. Relative humidity is initially assessed with respect to liquid water, and calculation necessary to convert raw values into relative humidity with respect to ice is performed according to Goff and Gratch (1945). As supersaturation is very unlikely at this coastal location notably due to frequent drifting snow, converted values exceeding 100 % are attributed to limitation of the conversion method and capped to 100 % (Barral et al., 2014).

Radiative fluxes designate the incoming shortwave radiation (SWD), outgoing shortwave radiation (SWU), incoming longwave radiation (LWD) and outgoing longwave radiation (LWU). All fluxes are defined positive when directed towards the surface. A Kipp and Zonen CNR4 net radiometer has been installed in early February 2014 next to the meteorological mast (Amory et al., 2020c). This sensor is composed by two pairs of pyrgeometers and pyranometers: the first one measures SWD and SWU (spectral range: 300 to 2800 nm) and the second one LWD and LWU (spectral range 4500 to 42000 nm). Sensor characteristics are presented in Table 1. Negative values of each radiation flux were set to 0. Summer maintenance operations and winter excessive discharge of the station's battery between May and September 2018 impacted measurement continuity. The later period was characterized by a gap of 55 % in the radiative flux observations. Outside this last time frame, few observations are missing as reported in Table 1.

Calculation of the turbulent heat fluxes, composed by the sensible heat flux (SHF) and the latent heat flux (LHF), could be possible with observations at D17 (relative humidity, temperature and wind speed) through the application of profile method

https://doi.org/10.5194/tc-2020-329
Preprint. Discussion started: 19 November 2020

(Barral et al., 2014). However, a first concern can be raised about the applicability of Monin–Obukhov similarity theory in drifting-snow conditions, as the requirement of vertical constancy in turbulent fluxes is not met (Bintanja, 2001; Amory and Kittel, 2019). Moreover, during drifting-snow occurrences, turbulent mixing and atmospheric sublimation favour the establishment of near-surface atmospheric layers characterized by low vertical gradients in humidity and temperature. Those gradients are frequently lower than the sensor accuracies, leading to large uncertainties in the derived turbulent fluxes. Barral et al. (2014) observed amplified uncertainty with strong winds at D17, furthermore limiting the use of the profile method during drifting-snow conditions. The same conclusion is drawn here, as determination of turbulent fluxes has been intended but led to strongly diverging results according to the choice of the method (bulk vs profile method), the stability function, the number and the considered height a.g.l. of the measurement levels (not shown). Thus, no observed turbulent fluxes are available here for model evaluation.

Information of drifting snow is obtained using second-generation IAV engineering FlowCapt sensors (hereinafter referred to as 2G-FlowCapt™, Amory et al. (2020a)). The 2G-FlowCapt™ is a 1 m long tube, containing an electroacoustic transducer measuring the noise generated by the impact of drifting-snow particles on the tube. The signal is then converted into a snow mass flux integrated over the exposed length of the tube. At D17, a pair of 2G-FlowCapt™ instruments has been operational since late December 2012. The sensors are set up vertically one above the other starting from the ground. This configuration enables for the detection of the initiation of drifting snow and measurement of the snow mass flux near the surface (< 2 m).

While the 2G-FlowCapt™ has been shown to underestimate snow mass fluxes compared to optical measurements in the French Alps (Trouvilliez et al., 2015), its behavior still needs to be assessed in the extreme Antarctic environment where different climatic conditions and particle properties influencing the measurement can be expected (Cierco et al., 2007). A preliminary evaluation of the 2G-FlowCapt™ instrument against optical measurements has been performed at D17 during one drifting-snow event and shows good agreement between both types of sensors (Amory, 2020). The lowest 2G-FlowCapt™ (respectively the highest), of exposed length h_1 (respectively h_2), measures a snow mass flux designated as FC_1 (respectively FC_2). Eq. 1 expresses the mean snow mass flux FC and takes into account the measurement height as accumulation can partially bury the lower 2G-FlowCapt™:

$$FC = \frac{h_1 \cdot FC_1 + h_2 \cdot FC_2}{h_1 + h_2} \quad (1)$$

All measurements are recorded every 15 s and mean values are performed every 30 min and stored on a Campbell CR3000 data logger.

2.2 Model description

MAR is a hydrostatic regional climate model solving primitive equations as originally described in Gallée and Schayes (1994), and extensively used for decade-long climate simulation over high-latitude regions (e.g., Agosta et al., 2019; Fettweis et al., 2017, 2020; Mottram et al., 2020; Kittel et al., 2020). Five atmospheric water species are represented in the model: specific humidity, cloud droplets, rain drops, cloud ice crystals, and snow particles (Gallée and Schayes, 1994). Radiative transfer

https://doi.org/10.5194/tc-2020-329
Preprint. Discussion started: 19 November 2020


The Cryosphere Discussions
Open Access
EGU

Table 1. Observed variables and technical specifications for sensors used at D17.

Variable	Sensor	Manufacturer	Accuracy	Observation period	Number of unaivailable data / All time steps
Wind speed	A100LK	Campbell scientific	$1\% \pm 0.1 m s{-}1$	2010-2018	<1 %
Relative Humidity	HMP45A	Vaisala	3 % for RH > 90 % 2 % for RH < 90 %	2010–2018	<1 %
Temperature	HMP45A	Vaisala	$\pm 0.4°$ C	2010-2018	<1 %
Snow height	Acoustic depth gauge SR50	Campbell scientific	± 0.01 m	2013-2018	<1 %
Snow mass flux	2G-FlowCapt™	IAV Engineering	Not specified	2013–2018	<1 %
Radiation	CNR4	Kipp and Zonen	5 % in daily totals	Feb. 2014–2018	6 %

through the atmosphere is calculated according to Morcrette (2002), and cloud radiative properties are calculated according to Ebert and Curry (1992) based on water species concentrations. MAR is coupled to the surface scheme SISVAT (Soil Ice Snow Vegetation Atmosphere Transfer; De Ridder and Gallée (1998); Gallée and Duynkerke (1997); Gallée et al. (2001)), which handles energy and mass transfer between the atmosphere and the surface, and includes a representation of snow properties (dendricity, sphericity and size) taken from an early version of the CROCUS snow model (Brun et al., 1992).

MAR includes a drifting-snow scheme originally described in Gallée et al. (2001). A detailed description of MARv3.11 latest version (including updates, changes relative to the original version and interactions with the surface and the atmosphere) can be found in Amory et al. (2020b). In brief, the drifting-snow scheme simulates erosion at every grid cell in which the modelled wind shear exceeds a threshold value depending on the local surface snow density. Once removed from the snowpack, eroded snow is mixed with the pre-existing windborne snow mass and advected to higher atmospheric levels and/or downwind grid cells by the turbulence and microphysical schemes. Interactions with the atmosphere are computed by the microphysical and the radiative transfer schemes. In particular, sublimation of suspended snow particles is modelled in each atmospheric level as a function of the air relative humidity according to Lin et al. (1983) and consequently modifies the local humidity budget, the lower atmosphere stratification and moist air advection. Representing the contribution of drifting-snow layers to the atmospheric radiative forcing is accounted for in MAR by including suspended snow particles in the computation of cloud radiative properties (Gallée and Gorodetskaya, 2010).

We used the latest model version MARv3.11 (hereinafter referred to as MAR) and setup as presented in Amory et al. (2020b), in which the model is run with a horizontal resolution of 10 km over a domain of 80 x 80 grid cells centered on D17 location. The atmosphere is described with 24 levels in the vertical, with a higher vertical resolution in the low troposphere. The first level is situated at 2 m above ground level (a.g.l.). Top-of-atmosphere and lateral forcing plus sea surface conditions are taken from 6-hourly ERA5-reanalysis (Hersbach et al., 2020). ERA5 products, evaluated in Antarctica by e.g. Gossart et al. (2017), notably assimilate radiosoundings operated every day at the closeby permanent station Dumont D'Urville, favouring a consistency between ERA5 and the observed climate in Adelie Land. Two models runs were performed with MAR over

https://doi.org/10.5194/tc-2020-329
Preprint. Discussion started: 19 November 2020

2010–2018. In the first run (referred to as MAR-DR), the drifting-snow scheme was activated oppositely to the second run (referred to as MAR-nDR).

2.3 Using CALIPSO to calculate drifting-snow height in MAR

Estimates of drifting-snow layer heights in MAR-DR are calibrated on CALIPSO observations. We underline the fact that satellite products are not used here for model evaluation, but rather as an independent product from which an objective criterion can be used to infer drifting-snow layer heights in our MAR simulations.

Palm et al. (2011) developed a remotely-sensed technique to detect drifting-snow properties and particularly the drifting-snow layer height. Lidar backscattered signal interaction with drifting snow is studied using the Cloud-Aerosol Lidar and Infrared Pathfinder Satellite Observations (CALIPSO) satellite. Under clear-sky condition, an algorithm, extensively detailed in Palm et al. (2011), analyzes the CALIPSO lidar attenuated backscatter signal over Antarctica and determines elevations of a scattering layer representative of the top of a drifting-snow layer. Such estimates enable drifting-snow detection for layers higher than 30 m. However, the snow particle ratio (the mass of snow particles per kg of air) at the top of the drifting snow layer, is not known.

The calibration algorithm works as follows: we firstly studied CALIPSO swaths above a 1 by 1 degree box centered on D17. When the satellite swath is covering this box and both MAR and the CALIPSO detection algorithm indicate a drifting-snow occurrence, the remotely-sensed drifting-snow layer height is retrieved. Then, the snow particle ratio (the mass of snow particles per kg of air at each model vertical level) from the closest vertical level in the MAR-DR simulation is stored (referred to as q_{s0}). Between January 2010 and October 2017, CALIPSO detected 56 distinct drifting-snow occurrences among the 462 observations available in the D17 area, giving q_{s0} values among which a mean snow particle ratio $\bar{q_{s0}}$ is computed. $\bar{q_{s0}}$, referred to as CALIPSO snow particle ratio threshold, is representative of the snow concentration required for the satellite to detect a drifting-snow layer. Secondly, all MAR-DR simulations are selected when drifting snow is simulated (i.e., when the snow mass flux at the lowest model level > $10^{-3}\,kg\,m^2\,s^{-1}$, calculated accordingly to Amory et al. (2015)). The highest vertical level with a snow particle ratio above $\bar{q_{s0}}$ corresponds to the drifting-snow layer height. In order to avoid accounting for modelled advected precipitation or snowflake atmospheric clouds as drifting-snow layers, data were filtered, according to the method described in Sect. 2.4. The model vertical discretization sets limits to the estimation of drifting-snow layer heights that are necessarily underestimated in MAR-DR if we consider CALIPSO-detected heights as a reference (drifting-snow height distributions are proposed in Supplementary material, Fig. S5).

2.4 Data Filtering

When drifting snow occurs, MAR computes radiative modifications related to both the presence of drifting-snow particles and the changes in the cloud representation. In Sect. 3.3, we focus on the radiative contribution of snow particles resulting from the erosion of the surface only, a task that required to filter the data.

Firstly, because cloud formation might be influenced by drifting snow through atmospheric sublimation and changes in the amount and distribution of atmospheric water species, it may induce radiative effects that are not directly related to drifting

https://doi.org/10.5194/tc-2020-329
Preprint. Discussion started: 19 November 2020

snow. The question of the role of the drifting snow on cloud formation cannot be supported here by enough observations and requires further investigations. Thus, we rejected all the cases where the increase in concentrations of cloud droplets, rain and ice crystals were among the 10 % highest increases between MAR-DR and MAR-nDR simulations.

Secondly, snowfall occurrence must be removed. Precipitating particles during snowfall can be distinguished between particles reaching the ground (designed as $\text{snowfall}_{\text{ground}}$) and particles sublimating entirely during their falling through the atmosphere (designed as $\text{snowfall}_{\text{virga}}$). As MAR-DR mixes $\text{snowfall}_{\text{ground}}$, $\text{snowfall}_{\text{virga}}$ and eroded snow particles in the snow particle ratio, we use the MAR-nDR simulation to discard $\text{snowfall}_{\text{ground}}$ and $\text{snowfall}_{\text{virga}}$ occurrences from both simulations. Once $\text{snowfall}_{\text{ground}}$ cases in MAR-nDR have been excluded, $\text{snowfall}_{\text{virga}}$ have been identified from the remaining cases in MAR-nDR (i.e. without $\text{snowfall}_{\text{ground}}$) as all profiles with a snow particle ratio above $q_{\text{snow0.9}}$ at any vertical level. $q_{\text{snow0.9}}$ is the 0.9 quantile of the snow particle ratio at the first vertical level. As a consequence, we rejected many snowfall occurrences, including drifting-snow mixed with snowfall occurrence and more generally many cloudy periods. Few single clear outliers remain after the filtering process (drifting-snow layer height > 2000 m) and are discarded.

Finally 13,853 simulated atmospheric profiles were available for analysis. Those profiles, designated as “filtered conditions”, hold valuable information about the direct radiative contribution of eroded snow particles without interfering with the radiative contribution of snowfall or newly formed atmospheric water species.

3 Results

The ability of MAR to reproduce the drifting-snow climate of Adelie Land has been extensively evaluated in Amory et al. (2020b), in which a close agreement with observations is demonstrated for the SMB, drifting-snow mass transport and frequency up to the scale of the drifting-snow event. We refer to this study for further details on the model evaluation regarding drifting snow. In this section, we focus on the impact of drifting snow on the representation of surface and near-surface meteorological variables. This is achieved by comparing two sets of simulations, in which the drifting-snow scheme has been respectively switched on (referred to as MAR-DR) and off (referred to as MAR-nDR). The results are compared over periods for which observations are also available, i.e. 2010–2018 for near-surface wind speed, air temperature and relative humidity and 2014-2018 for radiative fluxes. Except for the surface turbulent fluxes, all the other meteorological variables are observed at D17. Half-hourly variables extracted from the surface or the lowest model level (2 m) and the nearest grid cell to the observation location are used for comparison. Modifications in near-surface and surface variables are summarized in a Taylor Diagram (Taylor, 2001) presented in supplementary material (Fig. S1).

3.1 A case study

We firstly focus on a strong drifting-snow event that occured over the 1-3 October 2017 period at D17 to understand the physical processes involved in important changes between MAR-DR and MAR-nDR simulations.

https://doi.org/10.5194/tc-2020-329
Preprint. Discussion started: 19 November 2020

The Cryosphere Discussions
Open Access
EGU

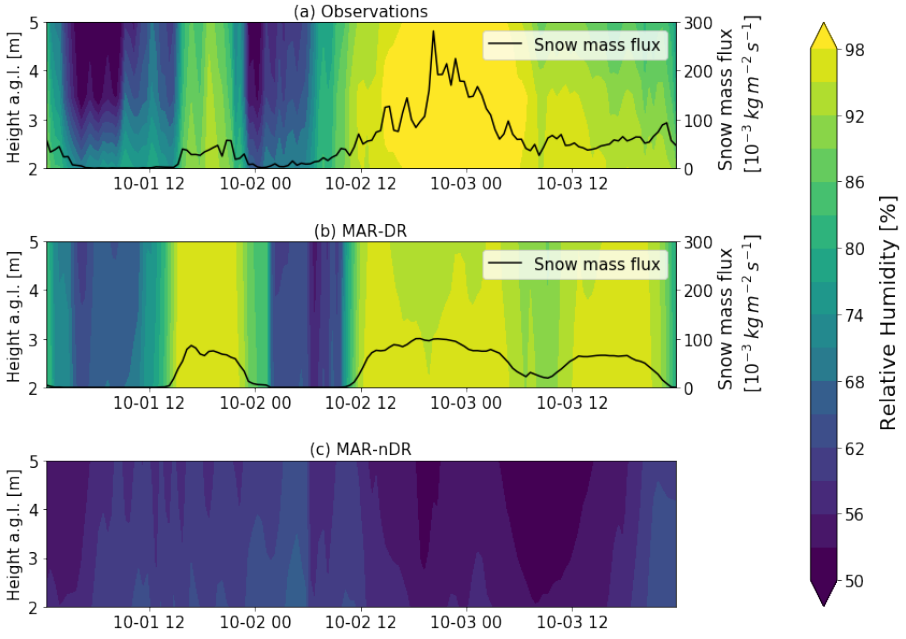

Figure 2. (a) Observed, (b) MAR-DR and (c) MAR-nDR vertical relative humidity profile (with respect to ice, color) and snow mass fluxes (from the surface to 2 m a.g.l., black line) between the 1st and the 3rd of October 2017.

3.1.1 Relative humidity, temperature and wind speed

MAR-DR captures the drifting-snow event in terms of timing and occurrence but underestimates the magnitude of the snow mass flux. The simulated drifting-snow flux is approximately three times lower than the observed flux at the peak of the event. The near-surface humidity budget is particularly impacted during this specific event (Fig. 2): when drifting snow occurs, a near-saturated layer develops in the lowest meters of the atmosphere. During the peak of the event, this layer reaches saturation. MAR-DR reproduces this observed increase in relative humidity, while relative humidity from MAR-nDR simulation is lower by up to 45 %.

As no snowfall is simulated during this event, the high snow particle ratio found in the lower part of the drifting-snow layer can be largely attributed to snow eroded from the surface by the wind (Fig. 3 (a)). Once suspended in the atmosphere, those particles sublimate in proportion to the undersaturation of ambient air (Schmidt, 1982) (Fig. 3 (b)), and relative humidity increases due to moisture release and consumption of latent heat and subsequent cooling of the atmosphere. This cooling decreases the 2 m temperatures (Fig. 3 (f)), also reducing the positive temperature bias in comparison to in-situ observations. A more complex behavior is observed for modifications in wind speed (Fig. 3 (h)), which are discussed in more detail in Sect. 4.1. Fig. S6 illustrates the impact of drifting snow on vertical profiles of temperature, relative humidity and wind speed in the model at D17 during this event where simulated profiles are consistent with mean vertical profiles, as discussed in Sect. 4.1.

https://doi.org/10.5194/tc-2020-329
Preprint. Discussion started: 19 November 2020

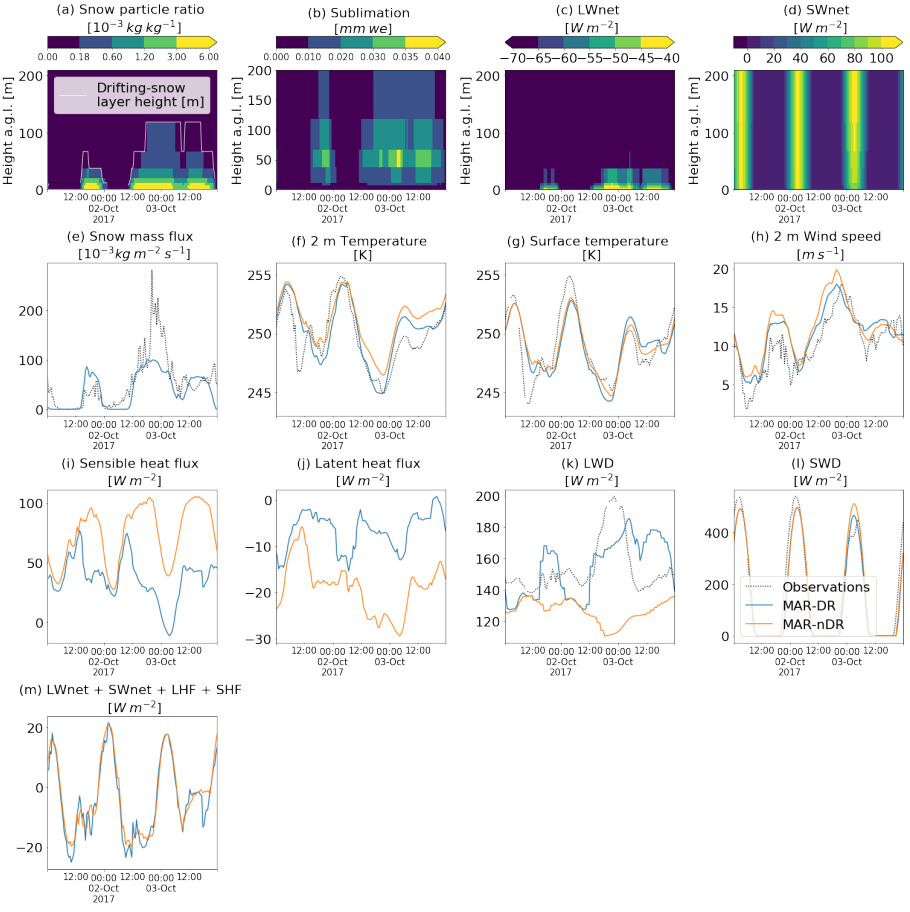

Figure 3. ((a) Snow particle ratio, (b) sublimation, (c) SWnet and (d) LWnet vertical profiles as simulated by MAR-DR during a drifting-snow episode occurring between the 1st and the 3rd of October 2017. (e) to (m): 2 m and surface variables as observed and simulated by MAR-DR and MAR-nDR between the 1st and the 3rd of October 2017.

3.1.2 Incoming radiative fluxes, turbulent fluxes and surface energy budget

During the 1-3 October 2017 period, both radiative and turbulent fluxes at the surface were modified by drifting snow. On the one hand, in MAR-DR during modelled drifting-snow occurrences, the net longwave radiation (LWnet), defined as LWD+LWU and calculated at each model vertical level, increases close to the surface and peaks where the snow particle ratio is maximum (Fig. 3 (c)). Conversely, the net shortwave radiation (SWnet), defined as SWD+SWU, decreases (Fig. 3 (d)). Those modifications are transferred towards the surface where large differences in LWD and SWD between MAR-DR and MAR-nDR are visible (Fig. 3 (k), (l)), suggesting the drifting-snow layer acts as a near-surface cloud by enhancing LWD and decreasing SWD at the surface. Yamanouchi and Kawaguchi (1984) observed similar LWD and SWD variations on the first 30 m of the atmosphere at Mizuho station during drifting-snow episodes.

https://doi.org/10.5194/tc-2020-329
Preprint. Discussion started: 19 November 2020

On the other hand, surface turbulent fluxes (not observed, see Sect. 2.1) is reduced when drifting snow is considered in the model (Fig. 3 (i), (j)). The development of a near-saturated layer on the first meters of the atmosphere due to drifting-snow sublimation (Fig. 2) reduces the humidity gradient and prevents surface sublimation with less latent heat exchange at the surface. Furthermore, atmospheric sublimation cools the atmosphere, inducing reduced vertical temperature gradients and lower sensible heat fluxes at the surface.

As a summary, we find that drifting snow induces a net radiative fluxes increase (+24.2 Wm^{-2} on average during the considered period), which is driven by increasing LWD and decreasing SWD. This compensates for turbulent fluxes modifications (-25.5 Wm^{-2}). Consequently, our simulations suggest that notable impacts on the energy inputs result in a negligible change in the final energy budget and surface temperature during this specific period.

3.2 Seasonal modifications

Drifting snow not only impacts the near-surface meteorology during specific events, but it also modifies their seasonal cycle at D17 (Fig. 4). As drifting snow becomes more frequent in winter (March to October) due to the increasing katabatic forcing (Amory et al., 2020b), its related impacts on the lower atmosphere are most notable during that period. As a result, relative humidity and LWD biases are notably reduced in winter in MAR-DR compared to MAR-nDR.

3.2.1 Relative humidity, temperature and wind speed

At 2 m above ground level, observations highlight a seasonal cycle in relative humidity (Fig. 4, (a)). MAR-DR captures this seasonal cycle, whereas MAR-nDR simulates nearly constant monthly means of relative humidity. As drifting-snow frequency and mass transport increase in winter Amory (2020), more airborne snow particles become available for sublimation. The lower temperatures in winter together with the additional atmospheric cooling and moistening caused by drifting-snow sublimation result in an increase in near-surface relative humidity. This sometimes leads to the establishment of a nearly saturated air layer over several meters (Fig. 2). Sublimation of airborne snow particles is responsible for a 13.9 % mean increase in 2 m relative humidity at D17 (2010–2018), which is consistent with previous simulations in this area (Lenaerts and van den Broeke, 2012). Taking into account drifting snow notably lowers the relative humidity root mean squared error (RMSE) by 31 % (Table 2), suggesting that drifting-snow sublimation mainly governs temporal variations in relative humidity at D17 in agreement with Amory and Kittel (2019).

Drifting snow also accounts for lower 2 m temperatures in MAR-DR at D17 (-0.6 K on average), particularly during winter (Fig. 4, (c)). However, further analysis shows that the most important temperature modifications occur higher up in the drifting-snow layer (Sect. 4.1). Accounting for drifting snow in MAR reduces the 2 m temperature positive bias in comparison with observations (divided by a factor 2, Table 2).

https://doi.org/10.5194/tc-2020-329
Preprint. Discussion started: 19 November 2020

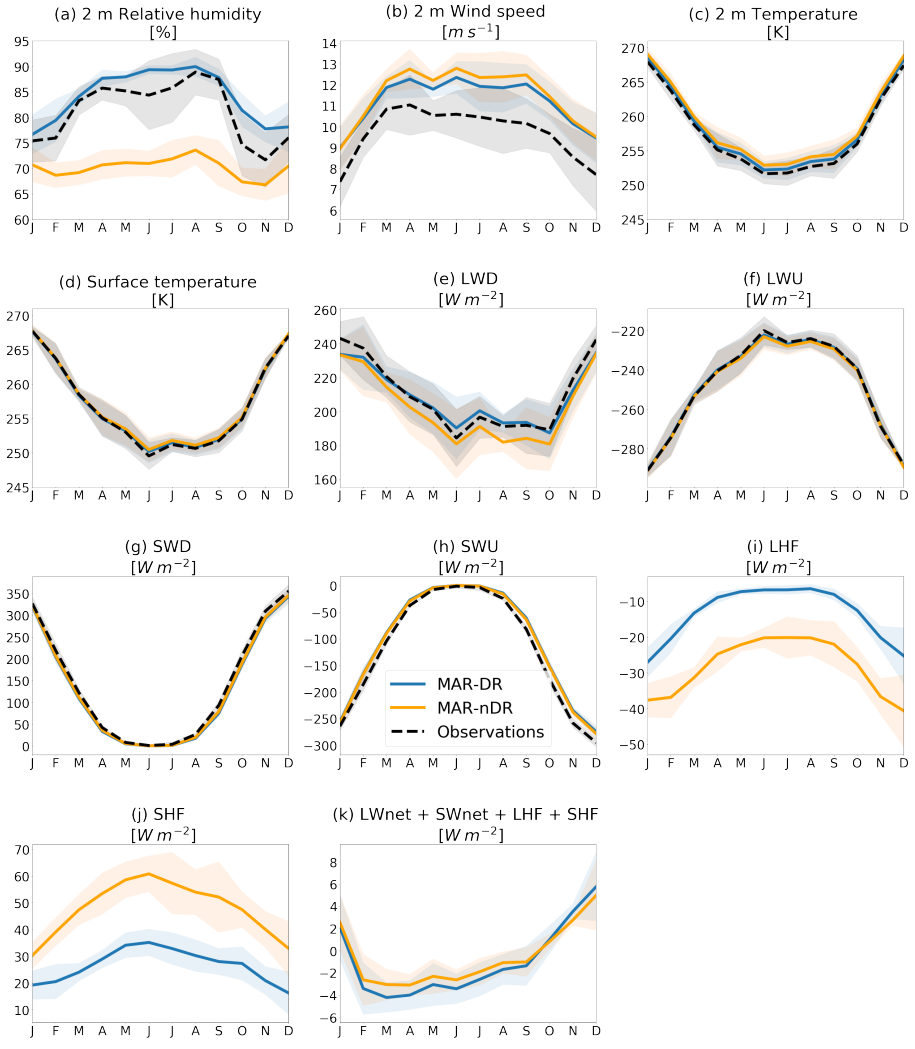

Figure 4. 2 m and near surface variable monthly means as simulated by MAR-DR and MAR-nDR. First, data are aggregated by both months and years. Then means and standard deviation are evaluated within each group aggregated by month. Statistics are performed on 2014–2018 period for radiative fluxes and surface temperature and on 2010–2018 period for near surface variables and turbulent fluxes.

https://doi.org/10.5194/tc-2020-329
Preprint. Discussion started: 19 November 2020


The Cryosphere Discussions

Table 2. Root mean square error (RMSE), Pearson correlation coefficient and mean bias computed at D17 for MAR-DR and MAR-nDR half-hourly simulations in comparison with in situ observations.

	r		RMSE		Mean bias	
	MAR-DR	MAR-nDR	MAR-DR	MAR-nDR	MAR-DR	MAR-nDR
LWD [Wm^{-2}]	0.88	0.89	16	17	-1.5	-7.6
LWU [Wm^{-2}]	0.97	0.98	5.6	5.2	0.2	0.9
SWD [Wm^{-2}]	0.98	0.98	5.6	5.2	0.2	0.9
SWU [Wm^{-2}]	0.97	0.98	24.2	23.4	-13.9	-12.3
Surface temperature [K]	0.97	0.97	1.4	1.4	0.1	0.3
2 m temperature [K]	0.97	0.97	1.4	1.6	0.6	1.2
2 m Wind speed []	0.80	0.82	2.5	2.6	1.5	1.8
2 m relative humidity [%]	0.59	0.51	9.7	14.2	2.9	-11.1

3.2.2 Incoming radiative fluxes, turbulent fluxes and surface energy budget

Drifting snow modifies the seasonal values of incoming radiative fluxes by enhancing LWD and decreasing SWD (Fig. 4 (e) and (g)). LWD are mainly modified during winter, in pace with the seasonal cycle of drifting snow. LWD modifications are even more visible during this period because atmospheric temperatures reach their minimum. As MAR-nDR underestimated LWD at D17 (the mean bias equals to -7.6 Wm^{-2}), the LWD negative bias is reduced to -1.5 Wm^{-2} in MAR-DR, showing that the latter simulates more realistic LWD values in winter. The impact of drifting snow on other incoming and outgoing radiative fluxes at the surface is lower (Table 2).

Drifting snow accounts for a significant decrease in SHF and LHF, i.e. larger than the interannual variability (taken as the standard deviation computed from annual means) during the 2010–2018 period. By increasing relative humidity in the lower atmosphere (Fig. 4 (a)), drifting-snow sublimation decreases the vertical gradient in humidity and limits latent heat exchanges with the surface. As a consequence, surface sublimation is locally reduced by a factor of 2.1 in MAR-DR (LHF, expressed in W m-2, Fig. 4(i)). However, at the same time, drifting-snow sublimation cools the boundary layer, reduces vertical temperature gradients and counterbalances the decrease in LHF by a decrease in SHF (Fig. 4 (j) (SHF divided by a factor 1.8 at D17).

Overall, drifting snow shows very little impact on the energy budget (LWnet + SWnet + LHF + SHF = -0.4 Wm^{-2}). This results from a compensation between the net drifting-snow radiative forcing (difference in SWnet + LWnet between simulations = 6.2 Wm^{-2}) and the surface turbulent heat fluxes (difference in LHF + SHF between simulations = -6.6 Wm^{-2}). As the energy available at the surface has not been notably modified by introducing drifting snow in MAR-DR, surface temperature is almost unchanged (-0.2 K, Fig. 4 (d)).

https://doi.org/10.5194/tc-2020-329
Preprint. Discussion started: 19 November 2020

The Cryosphere Discussions
Open Access
EGU

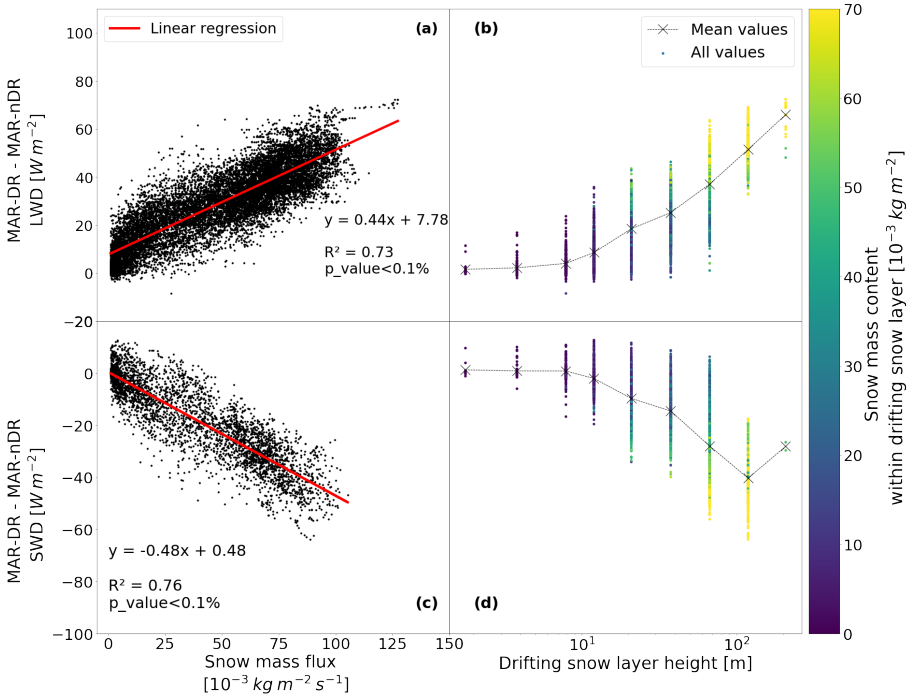

Figure 5. (a) and (c) Modifications in LWD and SWD between MAR-DR and MAR-nDR during drifting snow (near-surface snow mass flux > $10^{-3}\,kg m^2\,s^{-1}$), as a function of snow mass fluxes, for a mean flux calculated between 0 and 2m. The red line indicates the best linear regression between radiative modifications and snow ass fluxes. The grey shaded area corresponds to the root mean square error. Regression functions and statistics are displayed on the corresponding panels. SWD modifications are computed when MAR-nDR simulates SWD > 50 $W m^{-2}$. (b) and (d) Modifications in LWD and SWD between MAR-DR and MAR-nDR during drifting snow (snow mass flux >$10^{-3}\,kg m^2\,s^{-1}$), as a function of drifting-snow layer height. The colorbar indicates the mass of snow contained between the drifting-snow layer height and the surface. Mean values are calculated for the first 9 model vertical levels and are represented by a grey mark. SWD modifications are computed when MAR-nDR simulates SWD > 50 $W m^{-2}$.

3.3 Impact on incoming radiation

We intended analysing the impact of drifting snow on incoming radiation reaching the surface. In order to more specifically focus on the radiative contribution of eroded snow particles in MAR-DR, we filtered data according to Sect. 2.4 . Thus, we discarded cases with snowfall or modifications in the cloud structure between MAR-DR and MAR-nDR.

We observed that under such conditions, LWD modifications correlate linearly with the snow mass flux. Conversely, when significant SWD reaches the surface (> 50 $W m^{-2}$), SWD decreases linearly with the drifting-snow mass flux (Fig. 5 (a), (c)). Furthermore, large modifications in incoming radiative fluxes are associated with thick and dense drifting-snow layers (Fig. 5 (b), (d)).

https://doi.org/10.5194/tc-2020-329
Preprint. Discussion started: 19 November 2020

According to Fig. 5, the most significant drifting-snow events (snow mass fluxes >= $75\,10^{-3}\,kg\,m^2\,s^{-1}$ and layer height > 100 m) can lead to large increases in LWD: the largest increase occurs in October 2013 with + 72 Wm^{-2}. This effect is on average partially compensated by SWD decreases: the most notable decrease in SWD is reached in September 2010 with -64 Wm^{-2}. As suggested by our simulations, the net drifting-snow radiative forcing is positive (+ 6.2 Wm^{-2}, mean value on the all unfiltered dataset), particularly during filtered conditions (+ 26.2 Wm^{-2}), even when SWD are significant (+ 14.3 Wm^{-2}). The effect is more prominent during low solar irradiance periods because LWD is highly impacted whereas SWD is absent (or very low) and cannot be modified. The additional radiative forcing due to drifting snow is higher when eroded snow particles constitute the main part of suspended snow particles in the atmosphere.

Snow erosion and resulting drifting-snow sublimation modify the atmospheric composition in water species by introducing additional snow particles in the atmosphere and also enhancing its water vapor content, resulting in an increase in longwave emissivity (Yamanouchi and Kawaguchi, 1984). A sensitivity analysis was performed in order to distinct and quantify the relative contribution of eroded snow particles and additional water vapor to modified radiative fluxes. Additionally to MAR-DR and MAR-nDR, two other runs were performed for the year 2017, one similar to MAR-DR but not accounting for the radiative contribution of snow particles, the other one similar to MAR-nDR but not accounting neither for the radiative contribution of snow particles. The difference between the two last runs were compared to differences between MAR-DR and MAR-nDR for the year 2017 and demonstrated that incoming longwave modifications are predominantly due to the radiative contribution of drifting-snow particles (Fig. S2).

4 Discussion

4.1 Impact on the boundary layer

In the model at D17, the boundary layer is predominantly impacted on the first 600 m a.g.l. (first 11 vertical levels, Fig. 6). The snow particle ratio is high near the surface where snow erosion occurs, and decreases rapidly with height above the surface (Fig. 6 (j)). However, atmospheric sublimation peaks higher up (sixth MAR level, 38 m), as already suggested in e.g. van den Broeke et al. (2006) and Amory and Kittel (2019). As drifting-snow sublimation is a self-limiting process inhibited by the development of near-saturated layers close the the surface (Bintanja, 2001), the maximum in atmospheric sublimation during drifting-snow events occurs higher up in the atmosphere where sublimation is favoured by the under-saturation of the environment.

As observed by Palm et al. (2018) using dropsondes across Antarctica, well-mixed layers with small vertical gradients in temperature and increasing relative humidity with the proximity of the surface characterize the thermodynamic structure of drifting-snow layers. Fig. 6 shows that both features are reproduced by MAR, with a well-mixed temperature structure (< 0.015 Km^{-1}) within the first 100 m above ground, i.e. near the average height of drifting-snow layers, and a downward positive gradient in relative humidity. Further evaluation is however necessary to quantify the ability of the model to capture wind-shear-induced turbulent mixing and warm-air entrainment within katabatic flows.

According to the vertical profiles in Fig. 6, increases in wind speed, relative humidity, specific humidity and decreases in temperature are in accordance with increases in atmospheric sublimation. All of these variables are predominantly modified in

https://doi.org/10.5194/tc-2020-329
Preprint. Discussion started: 19 November 2020

The Cryosphere
Discussions
Open Access
EGU

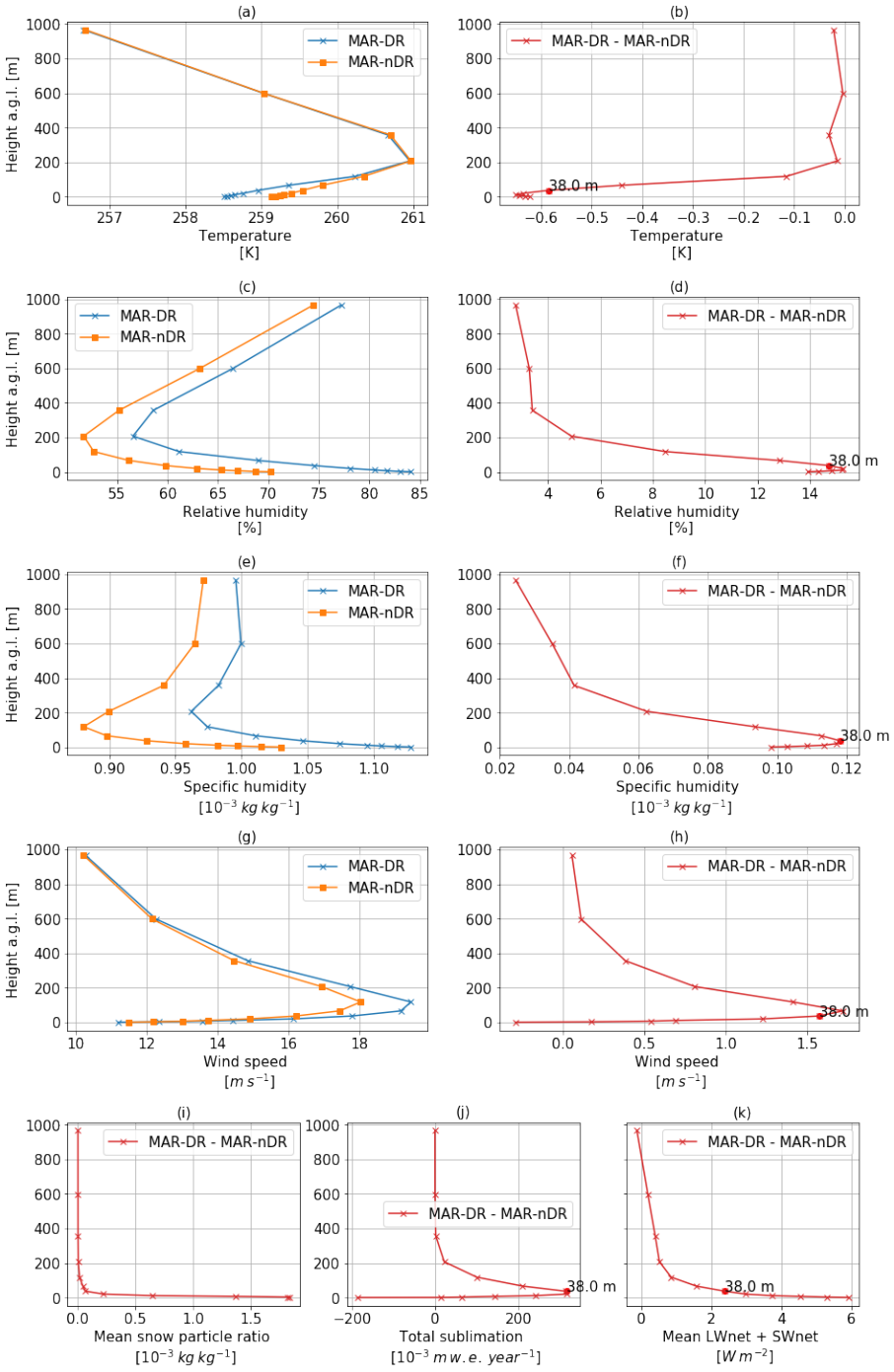

Figure 6. Mean vertical profiles for near-surface and surface variables calculated at D17 on the first 12 vertical levels as simulated by MAR-DR, MAR-nDR or corresponding differences between both runs. Note that (j) contains another level close to the surface indicating surface sublimation modifications between MAR-DR and MAR-nDR.

https://doi.org/10.5194/tc-2020-329
Preprint. Discussion started: 19 November 2020

the drifting-snow layer when accounting for drifting snow. The modification intensity peaks in the vicinity of the vertical level experiencing maximum atmospheric sublimation. This suggests that atmospheric sublimation drives the impacts of drifting snow on the low-atmosphere meteorology at D17. Accounting for this phenomenon at each vertical level modifies the entire boundary-layer structure.

Wind speed is on average lower in MAR-DR, in comparison with MAR-nDR, at the lowest vertical level (2 m) at D17. At all other vertical levels in the drifting-snow layer, wind speed is however oppositely higher in MAR-DR. Furthermore, increases in wind speed peak at the seventh vertical level, just above the level where mean atmospheric sublimation is maximum (fifth vertical model level, 38 m). As already suggested (e.g., Kodama et al., 1985), wind speed can increase during drifting snow events because of increased density of the air-snow mixture and an increased stable thermal stratification (Fig. 6 (a)) caused by the atmospheric sublimation-induced cooling (Bintanja, 2000). This effect is moderated at the first vertical model level by surface-atmosphere interactions, such as the consumption of turbulent kinetic energy required for removing snow particles from the surface and ensuring their maintenance in suspension.

Finally, we find that the net radiative budget (LWnet + SWnet) in the model vertical levels increases with the proximity of the surface within the drifting-snow layer (Fig. 6 (k)). This increase is due to suspended snow particles in the drifting-snow layer, which emit longwave radiation and trap heat, consequently inducing a warming effect that competes with cooling by sublimation. The comparison between MAR-DR and MAR-nDR suggests that the net effect is a decrease in atmospheric temperatures (Fig. 6 (a) and (b)), so the model suggests that the sublimation-induced cooling effect dominates.

4.2 Spatial analysis

By analysing our simulation at a regional scale, we demonstrate that the results obtained at D17 are distributed over coastal Adelie Land (Table 3).

Firstly, we estimate the drifting-snow magnitude at a regional scale by studying snow mass transport (Fig. 7 (a)). We calculate the mass of snow transported at the lowest atmospheric level at each grid point every year, and then calculate the annual mean values at each grid point. The spatial distribution of snow mass transport exhibits a close relationship with wind speed. It is particularly enhanced where the topographic slope accentuates and favours channeling of katabatic winds, initiated in the upper plateau region where wind speed and erosion are low.

The main drift-induced modifications in surface and near-surface variables described at D17 remain consistent at the scale of the integration domain. The spatial patterns of the differences in surface and near-surface variables correlate with spatial patterns of the snow mass transport as demonstrated by high and significant (p value < 0.01) Pearson correlation coefficient (Fig. 7). Modifications added by the drifting-snow scheme are often larger than the interannual variability (Fig. 7, undotted areas). However, surface temperature and melt modifications (not shown) are poorly linked with snow mass transport (respectively r=0.04 and r=0.3), another evidence that drifting snow does not modify the SEB significantly in the model.

We estimate the net drifting-snow radiative forcing on Adelie Land to be + 5.9 Wm^{-2} and the impact on SEB (estimated by LWnet + SWnet + LHF + SHF) to be smaller than 0.02 Wm^{-2}. Further spatial analysis performed at different vertical levels,

https://doi.org/10.5194/tc-2020-329
Preprint. Discussion started: 19 November 2020

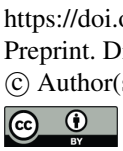

The Cryosphere Discussions
Open Access
EGU

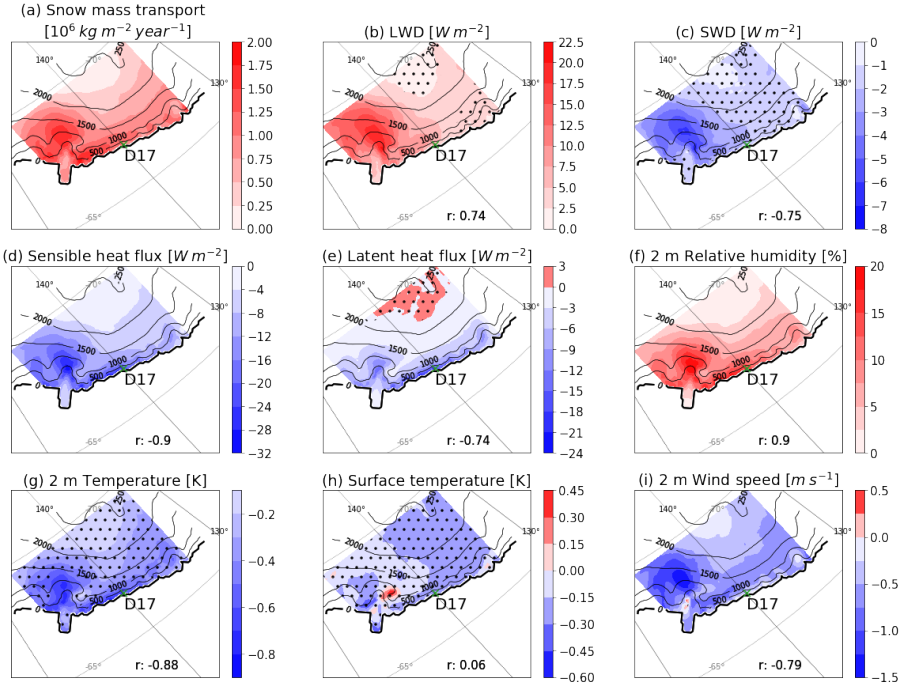

Figure 7. (a) Mean snow mass transported each year between the surface and 2m a.g.l. as simulated by MAR-DR. (b) to (i) Near-surface and surface variables modifications between MAR-DR and MAR-nDR on an integrative domain covering coastal Adelie Land. Within each panel, r indicates the Pearson correlation coefficient between snow mass transport (a) and the considered variable. Dotted area designate area where modifications are lower than interannual variability (taken as the standard deviation computed from annual means).

and shown in the supplementary material (Fig. S2), indicate that the drifting-snow impacts within the boundary layer simulated at D17 are also retrieved at a regional scale.

4.3 Comparing MARv3.11 and RACMOv2.1/ANT

Similarly to the approach adopted here, Lenaerts and van den Broeke (2012) already used the regional climate model RACMO2 to investigate the drifting-snow impact on the climate of Antarctica by comparing two distinct runs: one accounting for drifting snow, the other one not. Thus, we shed light on specific differences and similarities between our results with MARv3.11 and RACMO2.1/ANT as used in Lenaerts and van den Broeke (2012), by underlining specific and independent modeling approaches, sometimes leading to different impacts of drifting snow on the surface and the lower atmosphere.

Unlike with RACMO2.1/ANT, where latent heat exchanges for drifting-snow sublimation are computed in the surface energy budget (Lenaerts et al., 2012), MAR-DR simulates energy exchanges within each atmospheric layer in which sublimation occurs. Thus our simulations suggest that drifting-snow sublimation drives near-surface temperature decreases between MAR-DR and MAR-nDR. Oppositely Lenaerts and van den Broeke (2012) results suggest that drifting snow induces an increase in

https://doi.org/10.5194/tc-2020-329
Preprint. Discussion started: 19 November 2020


The Cryosphere Discussions

Table 3. Half-hourly mean value and standard deviation (STD) for several near-surface and surface meteorological variables computed on Adelie Land with MAR-DR and MAR-nDR. Differences between both model runs are attributed to drifting-snow processes.

	MAR-DR		MAR-nDR		|MAR-DR| - |MAR-nDR|	
	Mean value	STD	Mean value	STD	Mean value	STD
LWD [Wm^{-2}]	174.7	22.8	167.9	21.9	6.8	0.9
LWU [Wm^{-2}]	-209.7	22.4	-210.2	22.5	-0.5	-0.1
SWD [Wm^{-2}]	135.1	4.8	137.5	4.4	-2.4	0.4
SWU [Wm^{-2}]	-110.2	4.0	-111.2	3.6	-1.0	0.4
LHF [Wm^{-2}]	-2.2	2.7	-5.2	6.1	3.0	-3.4
SHF [Wm^{-2}]	12.0	3.6	21.0	8.5	-9.0	-4.9
LWnet + SWnet + LHF + SHF [Wm^{-2}]	-0.2	0.4	-0.2	0.3	0.0	0.1
Surface temperature [K]	245.9	6.7	246.0	6.7	-0.1	0
2 m temperature [K]	246.5	6.7	246.9	6.8	-0.4	-0.1
2 m wind speed [ms^{-1}]	9.6	1.6	10.2	1.8	-0.6	-0.2
2 m relative humidity [%]	94.4	2.7	88.3	5.8	6.1	-3.1

summer near-surface temperature. This increase is explained by the feedback between drifting snow and the surface state in RACMO2.1/ANT, which firstly lowers the surface albedo by sublimating surface snow and exposing older snow layers and secondly increases near-surface temperature with higher SWnet and surface temperatures. In MAR-DR, the erosion/deposition processes influence the albedo through modifications of the dendricity and sphericity of surface snow particles (Amory et al., 2020b). However no significant modification in surface albedo has been observed on the Adelie Land domain between MAR-DR and MAR-nDR. Quantitative comparisons between MAR and RACMO2 could enable to weight the impact of two distinct modeling approaches on near-surface temperature.

4.4 Limitations of the current evaluation method

Modifications in downwelling atmospheric radiation, induced by the inclusion of drifting snow in MAR, are consistent with former in situ estimates (Lesins et al., 2009; Mahesh et al., 2003; Yamanouchi and Kawaguchi, 1984; Yang et al., 2014) of the radiative contribution of suspended particles, suggesting the model simulates a realistic radiative forcing. However, our results might be affected, among other, by limitations in the vertical resolution of the model which does not take into account the large variations of snow particles concentration along the first 2 m of the low troposphere, and the limitations of the current radiative scheme (e.g., Delhasse et al., 2020), inherited from the ERA-40 reanalysis product (Uppala et al., 2005). Improved/regressed evaluation statistics when accounting for drifting snow can be linked with error compensation elsewhere in the model, independently from the ability of the model to accurately reproduce drifting-snow processes. Radiation measurements are scarce in Antarctica due to the harsh environmental conditions and the difficulty to deploy and maintain

https://doi.org/10.5194/tc-2020-329
Preprint. Discussion started: 19 November 2020

measurements sites in remote areas, thus more in situ observations of radiative fluxes and drifting-snow layer properties are needed for a more in-depth evaluation of model results and, in our case, assessment of the temporal and spatial representativity of the interactions described at site D17.

Including drifting snow in MAR shows large impacts on turbulent fluxes which compensate (and sometimes slightly override, e.g. at D17) modifications in radiative fluxes. Such a compensation needs to be evaluated through comparison with direct in situ measurements of latent and sensible heat fluxes during drifting-snow occurrences to determine if MAR-DR simulates (more) realistic turbulent heat exchanges at the surface.

5 Summary and conclusion

We investigated the impact of drifting snow on the low atmosphere and the surface in coastal Adélie Land by comparing two simulations, respectively with and without drifting snow, performed with the latest version of the regional climate model MAR (MARv3.11) over a 9-year-long period. Simulating drifting snow leads to notable modifications in near-surface and surface variables. Our results suggest such effects are mainly driven by additional sublimation of drifting-snow particles in the low-level atmosphere. Temperature decreases (-0.4 K on average, -0.6 K at D17) and relative humidity increases at 2 m a.g.l. (+6.1 % on average, +13.9 % at D17) when drifting snow is taken into account, as a result of the latent heat exchanges and the release of additional water vapor. Modifications in temperature and relative humidity are not largest at the surface where snow mass transport is the most intense, but peak higher in the drifting-snow layer at the fifth (21 m) atmospheric level in agreement with the magnitude of atmospheric sublimation.

Modifications in wind speed are dependent on the proximity to the surface: near the surface wind speed is reduced (-0.6 ms^{-1}), then it increases with elevation, by up to +1.2 ms^{-1} on average for the eighth vertical level at 119 m and +1.7 ms^{-1} on average at D17 at the seventh vertical level (67m). The largest increases also occur near the atmospheric level where atmospheric sublimation peaks. Thus, we observe a strong influence of drifting-snow sublimation on the structure of the boundary layer in the model, highlighting the importance of computing latent heat exchanges at each vertical level. When compared to in situ data observed at D17, 2 m relative humidity representation is greatly improved. The RMSE is reduced from 14.2 % to 9.7 % and the mean bias is reduced from -11.1 % to 2.9 %. Additionally, the 2 m temperature mean bias is also reduced (RMSE reduced from 1.6 K to 1.4 K, mean bias reduced from 1.2 K to 0.6 K).

We observe significant modifications in radiative and turbulent components of the SEB when taking into account drifting snow. The presence of a drifting-snow layer leads to modifications similar to the presence of a near-surface cloud, inducing enhanced LWD and decreased SWD. When the simulations are neither affected by snowfall nor drift-induced modifications in cloud structure (Sect. 2.4), we observed that the higher the snow drift content or the thicker the drifting-snow layers, the greater the modifications in radiative fluxes. As a result, LWnet increases at the surface (+7.3 Wm^{-2} on average), SWnet decreases (-1.4 Wm^{-2} on average), and the net effect is a positive drifting-snow radiative forcing of +5.9 Wm^{-2}. This is however mostly compensated in the drifting-snow layer by drifting-snow sublimation and at the surface by changes in turbulent fluxes. Atmospheric sublimation cools the lower atmosphere and reduces temperature and humidity gradients between the surface

https://doi.org/10.5194/tc-2020-329
Preprint. Discussion started: 19 November 2020

and the atmosphere, inducing less latent heat consumed and less sensible heat provided at the surface. The net effect between modification in LHF and SHF is less energy being provided at the surface (-5.9 Wm^{-2}). Consequently, we observed negligible impact on energy supply at the surface and no significant impacts on surface temperature between simulations.

As a consequence, this study shows that differences in terms of surface temperature and heat budget are limited between MAR-DR and MAR-nDR simulation. However, impacts on each energy flux are significant; changes are compensating each other. Consequently, calibrating MAR with surface temperature data would likely lead to similar scores in Antarctica for simulations accounting / not accounting for drifting snow processes. Nevertheless, drifting snow is a major component of both the surface mass balance and atmospheric moisture budget in the windy coastal area of Adelie Land (Amory and Kittel, 2019; Amory et al., 2020b). Thus accurately accounting for drifting snow improves the ability of the model to capture the atmospheric thermodynamics and interactions with the surface in a current climate. As air moisture, LWD, SHF and LHF could very likely vary in a changing climate, capturing drifting-snow processes is consequently a key for higher confidence in climate and surface mass balance projections. Furthermore, drifting snow induces modifications in the snow isotopic composition. Additionally to snow redistribution which alters stratigraphy measurements, drifting-snow sublimation, as a major contributor to the air moisture budget, scrambles relationships between water stable isotopes composition and climatic variables (Bréant et al., 2019). Improving quantification of modelled drifting snow and related sublimation is a first step before (i) implementing isotopes in MAR and (ii) improving uncertainty assessment for climate reconstructions (Landais et al., 2017).

As illustrated in Sect. 4.1, drifting snow modifies the low-atmosphere structure and thermodynamics. In particular, larger moisture content and higher relative humidity in the drifting-snow layer reduces the capacity of the low-level atmosphere to sublimate snow particles during snowfall (Grazioli et al., 2017), potentially impacting modelled snowfall rates at the surface. By increasing atmospheric moisture, drifting snow can also impact cloud formation and physical properties. Lenaerts and van den Broeke (2012) reported increasing snowfall when accounting for drifting snow with RACMO2.1/ANT in peripheral regions of the ice sheet, including coastal Adelie Land. As a consequence, drifting snow may have additional impact on the SEB and SMB. These additional processes have not been investigated in our study, mainly because MAR-DR in its current version does not discriminate between eroded and cloud-originating snow particles. Drift-induced modifications in cloud structure and precipitation would benefit further investigation, and are left for future work. Separating eroded snow from snowfall particles in the model could enable prescription of different particle properties and pave the way for improvements in the representation of the drifting-snow radiative forcing and more generally in the representation of the drifting-snow impact on the low-atmosphere and the ice-sheet surface.

Data availability. Radiation data are available at Amory et al. (2020c). Meteorological and drifting-snow data are available at Amory et al. (2020a). MAR simulations are freely available by contacting the authors.

https://doi.org/10.5194/tc-2020-329
Preprint. Discussion started: 19 November 2020

Author contributions. L.L.T., C.A. and V.F. designed the study. C.A. ran the simulations. L.L.T post-processed data, and wrote the first draft. C. A., C. K., X. F. and H. G. developped the model. V. K. processed CALIPSO data. C.A. and V.F collected field data. All authors contributed to the manuscript and discussed the results.

Competing interests. The authors declare that they have no conflict of interests.

Acknowledgements. This work would not have been possible without the financial and logistical support of the French Polar Institute IPEV (programme CALVA-1013 and GLACIOCLIM-SAMBA-411), and of the French Agence Nationale de la Recherche (projects ANR-14-CE01-0001 (ASUMA) and ANR-16-CE01-0011 (EAIIST)). The authors thank all the on-site personnel in Dumont d'Urville and Cap Prud'homme for their precious help in the field. Computational resources have been provided by the Consortium des Équipements de Calcul Intensif (CÉCI), funded by the Fonds de la Recherche Scientifique de Belgique (F.R.S. – FNRS) under grant no. 2.5020.11, and the Tier-1 supercomputer (Zenobe) of the Fédération Wallonie-Bruxelles infrastructure funded by the Walloon Region under grant agreement no. 1117545.

https://doi.org/10.5194/tc-2020-329
Preprint. Discussion started: 19 November 2020

References

Agosta, C., Amory, C., Kittel, C., Orsi, A., Favier, V., Gallée, H., van den Broeke, M. R., Lenaerts, J. T. M., van Wessem, J. M., van de Berg, W. J., and Fettweis, X.: Estimation of the Antarctic surface mass balance using the regional climate model MAR (1979–2015) and identification of dominant processes, The Cryosphere, 13, 281–296, https://doi.org/10.5194/tc-13-281-2019, 2019.

Amory, C.: Drifting-snow statistics from multiple-year autonomous measurements in Adélie Land, East Antarctica, The Cryosphere, 14, 1713–1725, https://doi.org/10.5194/tc-14-1713-2020, 2020.

Amory, C. and Kittel, C.: Brief communication: Rare ambient saturation during drifting snow occurrences at a coastal location of East Antarctica, The Cryosphere, 13, 3405–3412, https://doi.org/10.5194/tc-13-3405-2019, 2019.

Amory, C., Trouvilliez, A., Gallée, H., Favier, V., Naaim-Bouvet, F., Genthon, C., Agosta, C., Piard, L., and Bellot, H.: Comparison between observed and simulated aeolian snow mass fluxes in Adélie Land, East Antarctica, The Cryosphere, 9, 1373–1383, https://doi.org/10.5194/tc-9-1373-2015, 2015.

Amory, C., Genthon, C., and Favier, V.: A drifting snow data set (2010-2018) from coastal Adelie Land, Eastern Antarctica, https://doi.org/10.5281/zenodo.3630497, 2020a.

Amory, C., Kittel, C., Le Toumelin, L., Agosta, C., Delhasse, A., Favier, V., and Fettweis, X.: Performance of MAR (v3.11) at simulating the drifting-snow climate and surface mass balance of Adelie Land, East Antarctica, Geoscientific Model Development, submitted, 2020b.

Amory, C., Le Toumelin, L., Favier, V., and Genthon, C.: Radiation data (2014-2019) at site D17 (Adelie Land, East Antarctica), https://doi.org/10.5281/zenodo.4139737, 2020c.

Barral, H., Genthon, C., Trouvilliez, A., Brun, C., and Amory, C.: Blowing snow in coastal Adélie Land, Antarctica: three atmospheric-moisture issues, The Cryosphere, 8, 1905–1919, https://doi.org/10.5194/tc-8-1905-2014, 2014.

Bintanja, R.: On the glaciological, meteorological, and climatological significance of Antarctic blue ice areas, Reviews of Geophysics, 37, 337–359, https://doi.org/10.1029/1999RG900007, 1999.

Bintanja, R.: Snowdrift suspension and atmospheric turbulence. Part I: Theoretical background and model description, Boundary-Layer Meteorology, 95, 343–368, https://doi.org/10.1023/A:1002676804487, 2000.

Bintanja, R.: Snowdrift Sublimation in a Katabatic Wind Region of the Antarctic Ice Sheet, Journal of Applied Meteorology, 40, 1952–1966, https://doi.org/10.1175/1520-0450(2001)040<1952:SSIAKW>2.0.CO;2, 2001.

Brun, E., David, P., Sudul, M., and Brunot, G.: A numerical model to simulate snow-cover stratigraphy for operational avalanche forecasting, Journal of Glaciology, 38, 13–22, https://doi.org/10.3189/S0022143000009552, 1992.

Bréant, C., Leroy Dos Santos, C., Agosta, C., Casado, M., Fourré, E., Goursaud, S., Masson-Delmotte, V., Favier, V., Cattani, O., Prié, F., Golly, B., Orsi, A., Martinerie, P., and Landais, A.: Coastal water vapor isotopic composition driven by katabatic wind variability in summer at Dumont d'Urville, coastal East Antarctica, Earth and Planetary Science Letters, 514, 37 – 47, https://doi.org/10.1016/j.epsl.2019.03.004, 2019.

Cierco, F.-X., Naaim-Bouvet, F., and Bellot, H.: Acoustic sensors for snowdrift measurements: How should they be used for research purposes?, Cold Regions Science and Technology, 49, 74–87, https://doi.org/10.1016/j.coldregions.2007.01.002, 2007.

De Ridder, K. and Gallée, H.: Land Surface–Induced Regional Climate Change in Southern Israel, Journal of Applied Meteorology, 37, 1470–1485, https://doi.org/10.1175/1520-0450(1998)037<1470:LSIRCC>2.0.CO;2, 1998.

Delhasse, A., Kittel, C., Amory, C., Hofer, S., van As, D., S. Fausto, R., and Fettweis, X.: Brief communication: Evaluation of the near-surface climate in ERA5 over the Greenland Ice Sheet, The Cryosphere, 14, 957–965, https://doi.org/10.5194/tc-14-957-2020, 2020.

https://doi.org/10.5194/tc-2020-329
Preprint. Discussion started: 19 November 2020

Déry, S. J., Taylor, P. A., and Xiao, J.: The thermodynamic effects of sublimating, blowing snow in the atmospheric boundary layer, Boundary-Layer Meteorology, 89, 251–283, https://doi.org/https://doi.org/10.1023/A:1001712111718, 1998.

Ebert, E. E. and Curry, J. A.: A parameterization of ice cloud optical properties for climate models, Journal of Geophysical Research: Atmospheres, 97, 3831–3836, https://doi.org/10.1029/91JD02472, 1992.

Edwards, T. L., Brandon, M. A., Durand, G., Edwards, N. R., Golledge, N. R., Holden, P. B., Nias, I. J., Payne, A. J., Ritz, C., and Wernecke, A.: Revisiting Antarctic ice loss due to marine ice-cliff instability, Nature, 566, 58–64, https://doi.org/10.1038/s41586-019-0901-4, 2019.

Favier, V., Agosta, C., Genthon, C., Arnaud, L., Trouvillez, A., and Gallée, H.: Modeling the mass and surface heat budgets in a coastal blue ice area of Adelie Land, Antarctica, Journal of Geophysical Research: Earth Surface, 116, https://doi.org/10.1029/2010JF001939, 2011.

Favier, V., Krinner, G., Amory, C., Gallée, H., Beaumet, J., and Agosta, C.: Antarctica-regional climate and surface mass budget, Current Climate Change Reports, 3, 303–315, https://doi.org/10.1007/s40641-017-0072-z, 2017.

Fettweis, X., Franco, B., Tedesco, M., van Angelen, J. H., Lenaerts, J. T. M., van den Broeke, M. R., and Gallée, H.: Estimating the Greenland ice sheet surface mass balance contribution to future sea level rise using the regional atmospheric climate model MAR, The Cryosphere, 7, 469–489, https://doi.org/10.5194/tc-7-469-2013, 2013.

Fettweis, X., Box, J. E., Agosta, C., Amory, C., Kittel, C., Lang, C., van As, D., Machguth, H., and Gallée, H.: Reconstructions of the 1900–2015 Greenland ice sheet surface mass balance using the regional climate MAR model, The Cryosphere, 11, 1015–1033, https://doi.org/10.5194/tc-11-1015-2017, 2017.

Fettweis, X., Hofer, S., Krebs-Kanzow, U., Amory, C., Aoki, T., Berends, C. J., Born, A., Box, J. E., Delhasse, A., Fujita, K., Gierz, P., Goelzer, H., Hanna, E., Hashimoto, A., Huybrechts, P., Kapsch, M.-L., King, M. D., Kittel, C., Lang, C., Langen, P. L., Lenaerts, J. T. M., Liston, G. E., Lohmann, G., Mernild, S. H., Mikolajewicz, U., Modali, K., Mottram, R. H., Niwano, M., Noël, B., Ryan, J. C., Smith, A., Streffing, J., Tedesco, M., van de Berg, W. J., van den Broeke, M., van de Wal, R. S. W., van Kampenhout, L., Wilton, D., Wouters, B., Ziemen, F., and Zolles, T.: GrSMBMIP: Intercomparison of the modelled 1980–2012 surface mass balance over the Greenland Ice sheet, The Cryosphere Discussions, 2020, 1–35, https://doi.org/10.5194/tc-2019-321, 2020.

Gallée, H. and Gorodetskaya, I. V.: Validation of a limited area model over Dome C, Antarctic Plateau, during winter, Climate dynamics, 34, 61, https://doi.org/10.1007/S00382-008-0499-Y, 2010.

Gallée, H., Guyomarc'h, G., and Brun, E.: Impact of snow drift on the Antarctic ice sheet surface mass balance: possible sensitivity to snow-surface properties, Boundary-Layer Meteorology, 99, 1–19, https://doi.org/10.1023/A:1018776422809, 2001.

Gallée, H., Peyaud, V., and Goodwin, I.: Simulation of the net snow accumulation along the Wilkes Land transect, Antarctica, with a regional climate model, Annals of glaciology, 41, 17–22, https://doi.org/10.3189/172756405781813230, 2005.

Gallée, H. and Duynkerke, P. G.: Air-snow interactions and the surface energy and mass balance over the melting zone of west Greenland during the Greenland Ice Margin Experiment, Journal of Geophysical Research: Atmospheres, 102, 13 813–13 824, https://doi.org/10.1029/96JD03358, 1997.

Gallée, H. and Schayes, G.: Development of a Three-Dimensional Meso-γ Primitive Equation Model: Katabatic Winds Simulation in the Area of Terra Nova Bay, Antarctica, Monthly Weather Review, 122, 671–685, https://doi.org/10.1175/1520-0493(1994)122<0671:DOATDM>2.0.CO;2, 1994.

Gallée, H., Trouvilliez, A., Agosta, C., Genthon, C., Favier, V., and Naaim-Bouvet, F.: Transport of Snow by the Wind: A Comparison Between Observations in Adélie Land, Antarctica, and Simulations Made with the Regional Climate Model MAR, Boundary-Layer Meteorology, 146, 133–147, https://doi.org/10.1007/s10546-012-9764-z, 2013.

Goff, J. A. and Gratch, S.: Thermodynamic properties of moist air, Trans. ASHVE, 51, 125, 1945.

Gossart, A., Souverijns, N., Gorodetskaya, I. V., Lhermitte, S., Lenaerts, J. T. M., Schween, J. H., Mangold, A., Laffineur, Q., and van Lipzig, N. P. M.: Blowing snow detection from ground-based ceilometers: application to East Antarctica, The Cryosphere, 11, 2755–2772, https://doi.org/10.5194/tc-11-2755-2017, 2017.

Grazioli, J., Genthon, C., Boudevillain, B., Duran-Alarcon, C., Del Guasta, M., Madeleine, J.-B., and Berne, A.: Measurements of precipitation in Dumont d'Urville, Adélie Land, East Antarctica, The Cryosphere, 11, 1797–1811, https://doi.org/10.5194/tc-11-1797-2017, 2017.

Hanna, E., Pattyn, F., Navarro, F., Favier, V., Goelzer, H., van den Broeke, M. R., Vizcaino, M., Whitehouse, P. L., Ritz, C., Bulthuis, K., and Smith, B.: Mass balance of the ice sheets and glaciers – Progress since AR5 and challenges, Earth-Science Reviews, 201, 102 976, https://doi.org/10.1016/j.earscirev.2019.102976, 2020.

Hersbach, H., Bell, B., Berrisford, P., Hirahara, S., Horányi, A., Muñoz-Sabater, J., Nicolas, J., Peubey, C., Radu, R., Schepers, D., Simmons, A., Soci, C., Abdalla, S., Abellan, X., Balsamo, G., Bechtold, P., Biavati, G., Bidlot, J., Bonavita, M., De Chiara, G., Dahlgren, P., Dee, D., Diamantakis, M., Dragani, R., Flemming, J., Forbes, R., Fuentes, M., Geer, A., Haimberger, L., Healy, S., Hogan, R. J., Hólm, E., Janisková, M., Keeley, S., Laloyaux, P., Lopez, P., Lupu, C., Radnoti, G., de Rosnay, P., Rozum, I., Vamborg, F., Villaume, S., and Thépaut, J.-N.: The ERA5 global reanalysis, Quarterly Journal of the Royal Meteorological Society, 146, 1999–2049, https://doi.org/10.1002/qj.3803, 2020.

Hofer, S., Tedstone, A. J., Fettweis, X., and Bamber, J. L.: Decreasing cloud cover drives the recent mass loss on the Greenland Ice Sheet, Science Advances, 3, https://doi.org/10.1126/sciadv.1700584, 2017.

Hofer, S., Tedstone, A. J., Fettweis, X., and Bamber, J. L.: Cloud microphysics and circulation anomalies control differences in future Greenland melt, Nature Climate Change, 9, 523–528, https://doi.org/https://doi.org/10.1038/s41558-019-0507-8, 2019.

Kittel, C., Amory, C., Agosta, C., Delhasse, A., Doutreloup, S., Huot, P.-V., Wyard, C., Fichefet, T., and Fettweis, X.: Sensitivity of the current Antarctic surface mass balance to sea surface conditions using MAR, The Cryosphere, 12, 3827–3839, https://doi.org/10.5194/tc-12-3827-2018, 2018.

Kittel, C., Amory, C., Agosta, C., Jourdain, N. C., Hofer, S., Delhasse, A., Doutreloup, S., Huot, P.-V., Lang, C., Fichefet, T., and Fettweis, X.: Diverging future surface mass balance between the Antarctic ice shelves and grounded ice sheet, The Cryosphere Discussions, 2020, 1–29, https://doi.org/10.5194/tc-2020-291, 2020.

Kodama, Y., Wendler, G., and Gosink, J.: The Effect of Blowing Snow on Katabatic Winds in Antarctica, Annals of Glaciology, 6, 59–62, https://doi.org/10.3189/1985AoG6-1-59-62, 1985.

Landais, A., Casado, M., Prié, F., Magand, O., Arnaud, L., Ekaykin, A., Petit, J.-R., Picard, G., Fily, M., Minster, B., Touzeau, A., Goursaud, S., Masson-Delmotte, V., Jouzel, J., and Orsi, A.: Surface studies of water isotopes in Antarctica for quantitative interpretation of deep ice core data, Comptes Rendus Geoscience, 349, 139 – 150, https://doi.org/https://doi.org/10.1016/j.crte.2017.05.003, 2017.

Lenaerts, J. T. M. and van den Broeke, M. R.: Modeling drifting snow in Antarctica with a regional climate model: 2. Results, Journal of Geophysical Research: Atmospheres, 117, https://doi.org/10.1029/2010JD015419, 2012.

Lenaerts, J. T. M., van den Broeke, M. R., Déry, S. J., van Meijgaard, E., van de Berg, W. J., Palm, S. P., and Sanz Rodrigo, J.: Modeling drifting snow in Antarctica with a regional climate model: 1. Methods and model evaluation, Journal of Geophysical Research: Atmospheres, 117, https://doi.org/10.1029/2011JD016145, 2012.

Lesins, G., Bourdages, L., Duck, T. J., Drummond, J. R., Eloranta, E. W., and Walden, V. P.: Large surface radiative forcing from topographic blowing snow residuals measured in the High Arctic at Eureka, Atmospheric Chemistry and Physics, 9, 1847–1862, https://doi.org/10.5194/acp-9-1847-2009, 2009.

Lin, Y.-L., Farley, R. D., and Orville, H. D.: Bulk Parameterization of the Snow Field in a Cloud Model, Journal of Climate and Applied Meteorology, 22, 1065–1092, https://doi.org/10.1175/1520-0450(1983)022<1065:BPOTSF>2.0.CO;2, 1983.

Mahesh, A., Eager, R., Campbell, J. R., and Spinhirne, J. D.: Observations of blowing snow at the South Pole, Journal of Geophysical Research: Atmospheres, 108, https://doi.org/10.1029/2002JD003327, 2003.

Mann, G. W., Anderson, P. S., and Mobbs, S. D.: Profile measurements of blowing snow at Halley, Antarctica, Journal of Geophysical Research, 105, 24 491–24 508, https://doi.org/10.1029/2000JD900247, 2000.

Morcrette, J.-J.: Assessment of the ECMWF Model Cloudiness and Surface Radiation Fields at the ARM SGP Site, Monthly Weather Review, 130, 257–277, https://doi.org/10.1175/1520-0493(2002)130<0257:AOTEMC>2.0.CO;2, 2002.

Mottram, R., Hansen, N., Kittel, C., van Wessem, M., Agosta, C., Amory, C., Boberg, F., van de Berg, W. J., Fettweis, X., Gossart, A., van Lipzig, N. P. M., van Meijgaard, E., Orr, A., Phillips, T., Webster, S., Simonsen, S. B., and Souverijns, N.: What is the Surface Mass Balance of Antarctica? An Intercomparison of Regional Climate Model Estimates, The Cryosphere Discussions, 2020, 1–42, https://doi.org/10.5194/tc-2019-333, 2020.

Palm, S. P., Yang, Y., Spinhirne, J. D., and Marshak, A.: Satellite remote sensing of blowing snow properties over Antarctica, Journal of Geophysical Research: Atmospheres, 116, https://doi.org/10.1029/2011JD015828, 2011.

Palm, S. P., Kayetha, V., Yang, Y., and Pauly, R.: Blowing snow sublimation and transport over Antarctica from 11 years of CALIPSO observations, The Cryosphere, 11, 2555–2569, https://doi.org/10.5194/tc-11-2555-2017, 2017.

Palm, S. P., Kayetha, V., and Yang, Y.: Toward a Satellite-Derived Climatology of Blowing Snow Over Antarctica, Journal of Geophysical Research: Atmospheres, 123, 10,301–10,313, https://doi.org/10.1029/2018JD028632, 2018.

Scarchilli, C., Frezzotti, M., Grigioni, P., De Silvestri, L., Agnoletto, L., and Dolci, S.: Extraordinary blowing snow transport events in East Antarctica, Climate Dynamics, 34, 1195–1206, https://doi.org/10.1007/s00382-009-0601-0, 2010.

Schmidt, R.: Vertical profiles of wind speed, snow concentration, and humidity in blowing snow, Boundary-Layer Meteorology, 23, 223–246, https://doi.org/10.1007/BF00123299, 1982.

Shepherd, A., Ivins, E., Rignot, E., Smith, B., Van Den Broeke, M., Velicogna, I., Whitehouse, P., Briggs, K., Joughin, I., Krinner, G., et al.: Mass balance of the Antarctic Ice Sheet from 1992 to 2017, Nature, 558, 219–222, https://doi.org/10.1038/s41586-018-0179-y, 2018.

Taylor, K. E.: Summarizing multiple aspects of model performance in a single diagram, Journal of Geophysical Research: Atmospheres, 106, 7183–7192, https://doi.org/10.1029/2000JD900719, 2001.

Town, M. S., Walden, V. P., and Warren, S. G.: Cloud Cover over the South Pole from Visual Observations, Satellite Retrievals, and Surface-Based Infrared Radiation Measurements, Journal of Climate, 20, 544–559, https://doi.org/10.1175/JCLI4005.1, 2007.

Trouvilliez, A., Naaim-Bouvet, F., Genthon, C., Piard, L., Favier, V., Bellot, H., Agosta, C., Palerme, C., Amory, C., and Gallée, H.: A novel experimental study of aeolian snow transport in Adelie Land (Antarctica), Cold Regions Science and Technology, 108, 125–138, https://doi.org/10.1016/j.coldregions.2014.09.005, 2014.

Trouvilliez, A., Naaim-Bouvet, F., Bellot, H., Genthon, C., and Gallée, H.: Evaluation of the FlowCapt Acoustic Sensor for the Aeolian Transport of Snow, Journal of Atmospheric and Oceanic Technology, 32, 1630–1641, https://doi.org/10.1175/JTECH-D-14-00104.1, 2015.

Uppala, S. M., KÅllberg, P. W., Simmons, A. J., Andrae, U., Bechtold, V. D. C., Fiorino, M., Gibson, J. K., Haseler, J., Hernandez, A., Kelly, G. A., Li, X., Onogi, K., Saarinen, S., Sokka, N., Allan, R. P., Andersson, E., Arpe, K., Balmaseda, M. A., Beljaars, A. C. M., Berg, L. V. D., Bidlot, J., Bormann, N., Caires, S., Chevallier, F., Dethof, A., Dragosavac, M., Fisher, M., Fuentes, M., Hagemann, S., Hólm, E., Hoskins, B. J., Isaksen, L., Janssen, P. A. E. M., Jenne, R., Mcnally, A. P., Mahfouf, J.-F., Morcrette, J.-J., Rayner, N. A., Saunders, R. W.,

https://doi.org/10.5194/tc-2020-329
Preprint. Discussion started: 19 November 2020

Simon, P., Sterl, A., Trenberth, K. E., Untch, A., Vasiljevic, D., Viterbo, P., and Woollen, J.: The ERA-40 re-analysis, Quarterly Journal of the Royal Meteorological Society, 131, 2961–3012, https://doi.org/10.1256/qj.04.176, 2005.

van den Broeke, M., van de Berg, W. J., van Meijgaard, E., and Reijmer, C.: Identification of Antarctic ablation areas using a regional atmospheric climate model, Journal of Geophysical Research: Atmospheres, 111, https://doi.org/10.1029/2006JD007127, 2006.

van Wessem, J. M., van de Berg, W. J., Noël, B. P. Y., van Meijgaard, E., Amory, C., Birnbaum, G., Jakobs, C. L., Krüger, K., Lenaerts, J. T. M., Lhermitte, S., Ligtenberg, S. R. M., Medley, B., Reijmer, C. H., van Tricht, K., Trusel, L. D., van Ulft, L. H., Wouters, B., Wuite, J., and van den Broeke, M. R.: Modelling the climate and surface mass balance of polar ice sheets using RACMO2 – Part 2: Antarctica (1979–2016), The Cryosphere, 12, 1479–1498, https://doi.org/10.5194/tc-12-1479-2018, 2018.

Yamanouchi, T. and Kawaguchi, S.: Longwave radiation balance under a strong surface inversion in the Katabatic Wind Zone, Antarctica, Journal of Geophysical Research: Atmospheres, 89, 11 771–11 778, https://doi.org/10.1029/JD089iD07p11771, 1984.

Yang, Y., Palm, S. P., Marshak, A., Wu, D. L., Yu, H., and Fu, Q.: First satellite-detected perturbations of outgoing longwave radiation associated with blowing snow events over Antarctica, Geophysical Research Letters, 41, 730–735, https://doi.org/10.1002/2013GL058932, 2014.